Journal of Fluorescence, Vol. 2, No. 2, 1992

Fluorescence Intensity and Anisotropy Decay of the 4′,6-Diamidino-2-phenylindole–DNA Complex Resulting from One-Photon and Two-Photon Excitation

Joseph R. Lakowicz[1] and Ignacy Gryczynski[1]

Received April 3, 1992; revised July 10, 1992; accepted July 15, 1992

We examined the emission spectra, intensity decays, and anisotropy decays of the DNA–4′,6-diamidino-2-phenylindole (DAPI) complex resulting from one- and two-photon excitation of fluorescence. Similar lifetimes and correlation times were recovered from the frequency-domain data. However, the initial anisotropies of DAPI for one- and two-photon excitation revealed different angles between the absorption and the emission oscillators, 17.8 and 23.8°, respectively. This suggests the presence of two overlapping transitions in DAPI with different one- and two-photon cross sections for absorption.

KEY WORDS: 4′,6-Diamidino-2-phenylindole–DNA complex; fluorescence intensity; anisotropy decay; one- and two-photon excitation.

INTRODUCTION

The stain 4′,6-diamidino-2-phenylindole (DAPI) binds to DNA with a significant increase in fluorescence [1–5]. Consequently, DAPI is widely used for selective visualization of DNA in fluorescence microscopy, flow cytometry, and chromosome analysis. While there is some controversy over whether the positively charged DAPI molecule binds to DNA by electrostatic or intercalative interactions, there is agreement that the extent of fluorescence enhancement is largest for binding to AT base pairs, with minimal enhancement by GC pairs [6–9]. Time-resolved studies of DAPI–DNA complexes have revealed longer decay times for polyd(AT) and polyd(A)–polyd(T) than for calf thymus DNA or polyd(GC) [8,9]. The fluorescence intensity decays of DAPI–DNA complexes are somewhat heterogeneous, which has been interpreted as the result of multiple solvation states of the DNA [9] or the presence of various ionization states of DAPI at neutral pHs [10].

We have not attempted to dissect further the detailed spectroscopic properties of the DAPI–DNA complex, which we accept as important in the use of this valuable DNA probe. In the present report we consider the growing use of two-photon excitation (TPE) in analytical chemistry [11], spectroscopy of biomolecules [12–16], and fluorescence microscopy [17–19]. In the latter application, the use of TPE results in an intrinsic ability to obtain confocal fluorescent images [17]. This fact, and the growing interest in fluorescence lifetime imaging [20–22], makes it of interest to examine the decay characteristics of the DAPI–DNA complex for one- and two-photon excitation (OPE and TPE) of fluorescence.

MATERIALS AND METHODS

Calf thymus DNA from Sigma and DAPI from Molecular Probes were used without further purification. To avoid aggregation and increase total solubility, the

[1] Center of Fluorescence Spectroscopy, Department of Biological Chemistry, University of Maryland, School of Medicine, 660 West Redwood Street, Baltimore, Maryland 21201.

1053-0509/92/0600-0117$06.50/0

DNA was sonicated for 10 min in an ice bath, followed by centrifugation for 30 min at 10,000 rpm to particles. The buffer was 10 m*M* Tris, pH 8. The DNA concentration, as millimolar base pairs (bp), was calculated using 13,500 M^{-1} cm^{-1} at 259 nm, and the concentration of DAPI was calculated using 33,000 M^{-1} cm^{-1} at 345 nm for the free form (from the Molecular Probes catalogue). The extinction coefficient decreases in binding to DNA [23].

To facilitate comparison of the data, the OPE and TPE experiments were performed on the same solution, containing 10 m*M* bp of DNA and 0.2 m*M* DAPI, for a 50/1 bp/DAPI ratio. Under these conditions, all the DAPI appears to be bound and the intensity decays are independent of the bp/DAPI ratio [5,8,9]. The concentration of DAPI in glycerol was 0.2 m*M*.

OPE was accomplished using the frequency-doubled output of a cavity-dumped pyridine 2 laser at 360 nm. For TPE we used the fundamental output at 720 nm, which was focused in the sample using a 5-cm-focal length lens. For both OPE and TPE, the pulse width was about 5 ps at a repetition rate of 3.795 MHz. For the frequency-domain intensity and anisotropy decays, the emission was observed through a combination of 4-96 and 3-75 Corning filters. Signal from the solvent alone was less than 0.5% for both OPE and TPE. Steady-state anisotropy data were obtained using the usual L-format configuration [24].

Because of the high absorbance of DAPI, it was not possible to use the usual right-angle geometry with the focal point in the center of the cuvette. For OPE, we used a 0.5 × 0.5-cm cuvette, which was positioned off center in a 1 × 1-cm cuvette holder so that excitation and emission were located near the front corner. For TPE, we used 1.0 × 0.5-cm cuvettes, with the long axis aligned along the incident light path and with the focal point positioned about 0.5 cm from the surface facing the incident light.

Frequency-domain intensity and anisotropy decays were obtained on the GHz instrument described previously [25,26]. Intensity decays were measured using magic-angle conditions. Intensity decays [$I(t)$] were fit to a multiexponential model using

$$I(t) = \sum_i \alpha_i e^{-t/\tau_i} \tag{1}$$

where α_i are the amplitudes associated with the decay time τ_i. The mean decay time $\langle\tau\rangle$ is given by $\langle\tau\rangle = \sum_i \alpha_i\tau_i^2 / \sum_i \alpha_i\tau_i$. The differential phase and modulated anisotropy data were fit to the multicorrelation time anisotropy decay [$r(t)$] model using

$$r(t) = \sum_j r_{0j} e^{-t/\tau_i} \tag{2}$$

where r_{0j} is the fraction of the total anisotropy ($r_0 = \sum_i r_{0j}$) which decays with a correlation time θ_j.

THEORY

In previous reports [27,28] we examined OPE and TPE anisotropy spectra of molecules with collinear absorption and emission dipoles. The experiments were consistent with a $\cos^4\theta$ dependence of the absorption probability, where θ is the angle between the absorption dipole and the electric vector of the polarized excitation. The $\cos^4\theta$ dependence is distinct from the $\cos^2\theta$ dependence for OPE [32]. Consequently, TPE results in a more highly oriented photoselected population if the OPE and TPE transition moments are collinear [27,28]. Suppose the fluorophores do not undergo rotational diffusion during the time between excitation and emission or that one measures the anisotropy at time = 0. Then, for randomly oriented solution, excited with vertically polarized light, the absorption probabilities result in anisotropy values which are given by

$$r^1(\beta) = \frac{2}{5}\left(\frac{3}{2}\cos^2\beta_1 - \frac{1}{2}\right) \tag{3}$$

and

$$r^2(\beta) = \frac{4}{7}\left(\frac{3}{2}\cos^2\beta_2 - \frac{1}{2}\right) \tag{4}$$

where the superscripts 1 and 2 refer to OPE and TPE, respectively, and β_i is the angle between the absorption and the emission transition moments. For collinear OPE and TPE transitions $\beta_1 = \beta_2$. Equation (4) has been derived in our earlier publications on this topic [27,28]. This equation can also be obtained on the basis of photoselection theory for simultaneous two-photon absorption [29,30] or as two sequential one-photon absorptions [31], in both cases assuming that the second transition is parallel to the first and no depolarization occurs in the virtual and/or intermediate states.

We investigated the dependence of β on the mode of excitation in two ways. DAPI itself was examined in vitrified glycerol, in which case the steady-state anisotropy values can be interpreted in terms of β_i using Eqs. (3) and (4). For the DAPI–DNA complex, we used the total anisotropy recovered from the multicorrelation time

analysis [Eq. (2)] of the frequency-domain anisotropy data, which again yields β_i using the value of r_0 and Eqs. (3) and (4). The values of β were also recovered directly by formulating the anisotropy least-squares algorithm in terms of β. This approach also allows global analysis of the OPE and TPE to determine whether both types of data could be interpreted in terms of a single value of β. In this global analysis, it is assumed that the TPE excitation anisotropy values are 10/7 larger than the OPE values [Eqs. (3) and (4)], which is equivalent to assuming $\beta_1 = \beta_2$.

RESULTS

Emission Spectra of the DAPI–DNA Complex

Emission spectra of DAPI–DNA are shown in Fig. 1. The same emission spectra were observed for OPE (---) and TPE (—). Since the decay kinetics of DAPI may depend on the emission wavelengh, at least for the free dye [10], the transmission profile of the chosen emission filter combination is shown in Fig. 1 (· · ·). The DAPI emission was quadradically dependent (inset) on the incident intensity at 720 nm (•) but linearly dependent on intensity at 360 nm (○). In the inset the emission intensities were normalized to unity for the maximum excitation intensity. This quadratic intensity dependence is strong evidence that the observed emission was in fact due to simultaneous absorption of two photons at 720 nm [15,33–35].

Fluorescence Intensity Decays of DAPI–DNA

Frequency responses for the total DAPI emission from DAPI–DNA are shown in Fig. 2 for OPE at 360 nm (○; top) and TPE at 720 nm (•; bottom). These frequency responses are nearly identical, as are the α_i and τ_i values from the multiexponential fit (Table I), suggesting that emission occurs from the same state independent of the mode of excitation.

Frequency-Domain Anisotropy Decays of DAPI–DNA

The frequency-domain anisotropy data are distinct for OPE and TPE of DAPI–DNA (Fig. 3). The differential phase and modulated anisotropy values are higher for TPE (•) than for OPE (○). This effect is reminiscent of our previous results for diphenylhexatriene (DPH) [27] and 2,5-diphenyloxazole (PPO) [28]. However, in contrast to DPH and PPO, the r_0 values from the anisotropy decay analysis are not linked by the relative photoselection factor of 10/7 predicted by Eqs. (3) and (4). Stated alternatively, the anisotropy decay analysis does not yield the same values of β for OPE and TPE (Table II), whereas the correlation times are similar. This suggestion of different values of β_1 and β_2 is supported by an attempt to fit the OPE and TPE data using a single global value of β. This attempt results in an unacceptable fit (Fig. 3; ---) and a 210-fold elevation in χ^2_R, providing strong evidence for different values of β_1 and β_2. Nonetheless, we examined the χ^2_R surfaces for β_1 and β_2 to determine if

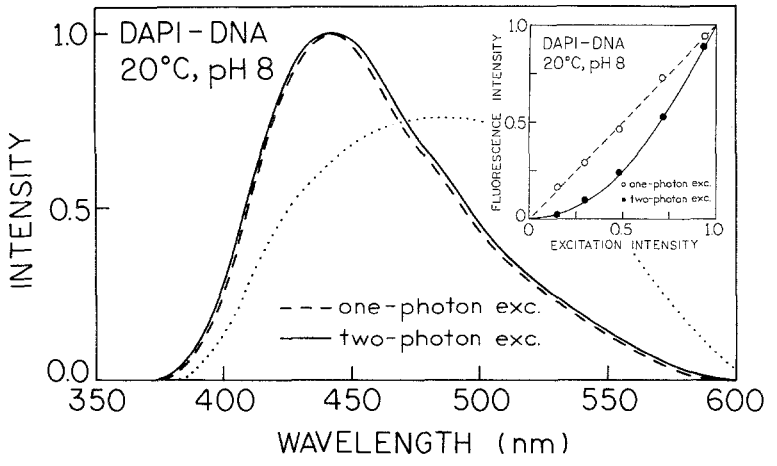

Fig. 1. Fluorescence emission spectra for OPE (---; 360 nm) and TPE (—; 720 nm) of DAPI–DNA. The dotted line shows the transmission profile of the emission filter combination Corning 4-96 and 3-75. The inset shows the dependence of the maximum intensity on the incident light level.

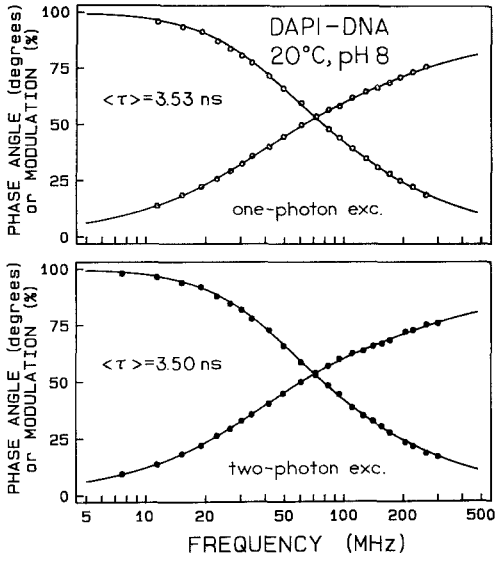

Fig. 2. Frequency-domain intensity decays of DAPI-DNA for OPE (○; top) and TPE (●; bottom).

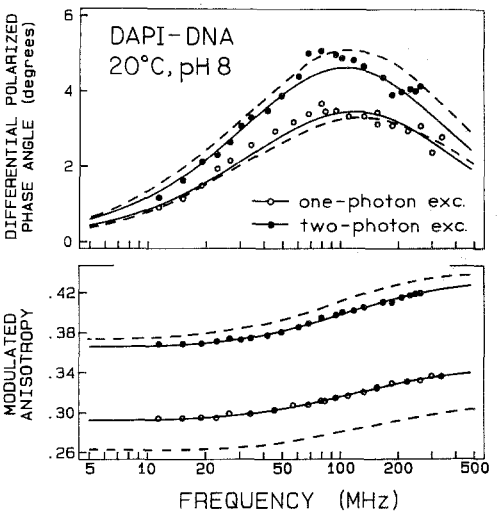

Fig. 3. Frequency-domain anisotropy data for OPE (○) and TPE (●) of DAPI-DNA. The dashed line shows the best global fit to the OPE and TPE data using a single value of β.

Table I. Multiexponential Analysis of the DAPI-DNA Fluorescence Intensity Decays

Excitation	$\langle\tau\rangle$ (ns)[a]	τ_i (ns)	α_i	f_i	χ^2_R
360 nm		1.25	0.351	0.147	
(OPE)	3.53	3.93	0.649	0.853	2.1
720 nm		0.98	0.303	0.101	
(TPE)	3.50	3.78	0.697	0.899	2.3

[a] $\langle\tau\rangle = \sum_i f_i\tau_i = \sum_i \alpha_i\tau_i^2 / \sum_i \alpha_i\tau_i$.

Table II. Multicorrelation Time Analysis of the DAPI-DNA Complex

Excitation	β_i (deg)	$r_0 g_i$	θ_i (ns)	χ^2_R
360 nm	17.8	0.062	1.59	1.3
OPE		0.282	93.87	
720 nm	23.8	0.077	1.65	
TPE		0.356	74.01	2.9
Global, 1β	22.1	0.052; 0.074	1.2	
(OPE; TPE)		0.263; 0.376	56.3	431.1
global, 2β	17.8; 23.7	0.062; 0.078	1.63	2.2
(OPE; TPE)		0.282; 0.355	79.52	

there was a correlation between the parameters [r_0 and θ_j in Eq. (2)]. These χ^2_R surfaces (Fig. 4) demonstrate that the OPE data are not consistent with β_2 and that the TPE data are not consistent with β_1. Hence, the analysis indicates that β_1 and β_2 are clearly different for OPE and TPE of fluorescence.

Anisotropy Excitation Spectra of DAPI in Glycerol

Estimation of the initial (time = 0) anisotropy from the frequency-domain data is subject to error due to the limited time resolution of all such measurements [36,37]. Hence, we examined the steady-state anisotropy of DAPI itself in glycerol at −30°C (Fig. 5). These data reveal at 34% increase in r_0 for TPE, comparable to the 26% increase seen from the time-resolved data (Table II). Hence, these different measurements of r_0 are in agreement, and in the case of DAPI–DNA and DAPI in glyc-

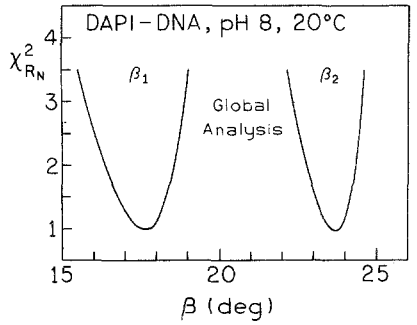

Fig. 4. The χ^2_R surface for the angles β_1 and β_2 in Eqs. (3) and (4), for OPE and TPE of DAPI–DNA, respectively.

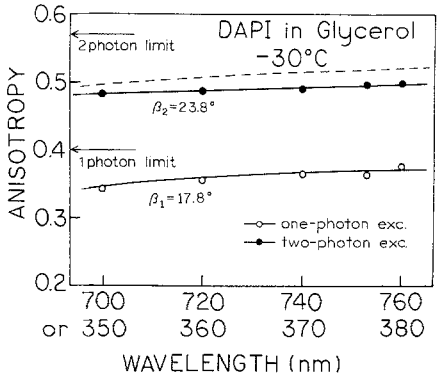

Fig. 5. Excitation anisotropy spectra of DAPI in glycerol, −30°C. The upper, dashed line shows the anisotropy values expected for an increased TPE photoselection factor of 10/7.

erol, the TPE anisotropy is not 10/7-fold or 43% larger than the OPE anisotropy, as one would expect if the β values were identical for OPE and TPE.

DISCUSSION

What is the meaning of the different apparent values of β for OPE and TPE? To date, we have observed nearly identical values of β for 2,5-diphenyloxazole [28] and 1,6-diphenylhexatriene [27] but very different values of β for indole [38] and the single tryptophan residue in HSA [16]. In general, the two-photon tensor may have additional terms within a single electronic transion, resulting in different apparent values of β for OPE and TPE. However, in this case of indole and HSA, it seems likely that the different values of β are the result of different relative cross sections for OPE and TPE of the ^1L_a and ^1L_b transitions of indole. Since emission from indole and proteins in polar solvents occurs from the ^1L_a state, and the ^1L_a and ^1L_b transitions are perpendicular, changes in the relative absorption of these states will alter the measured anisotropy. This interpretation, while rational, is currently unproven. In the case of DAPI, the OPE and TPE transition appears to have similar but not identical orientations within the molecular frame, suggesting that at least two electronic transitions contribute to the absorbance at 360 and 720 nm. This is not surprising given the structural similarity of DAPI and indole.

And finally, we note that these data may be valuable in the interpretation of lifetime measurements in fluorescence microscopy [19–22]. Based on our results, identical decay times can be expected for OPE and TPE and the anisotropy decay should display a 26 to 34% increased amplitude for TPE.

ACKNOWLEDGMENTS

The authors acknowledge support from the National Science Foundation (DMB-8804931 and DIR-8710401), the National Institutes of Health (RR-04800 and RR-07510), and the Medical Biotechnology Center and Graduate School at the University of Maryland. We thank Dr. Badri Maliwal for his assistance with the preparation of the samples and Drs. Józef Kuśba and Michael L. Johnson for providing the needed software.

REFERENCES

1. J. Kapuscinski and B. Skoczylas (1978) *Nucleic Acids Res.* **5,** 3775–3799.
2. L. Masotti, P. Cavatorta, M. Avitabile, M. L. Barcellona, J. von Berger, and N. Ragusa (1982) *Ital. J. Biochem.* **31,** 90–99.
3. J. Kapuscinski and W. Szer (1979) *Nucleic Acids Res.* **6,** 3519–3535.
4. L. Masotti, M. L. Barcellona, J. von Berger, and M. Avitabile (1981) *Biosci. Rep.* **1,** 701–707.
5. P. Cavatorta, L. Masotti, and A. G. Szabo (1985) *Biophys. Chem.* **22,** 11–16.
6. M. S. Lin, D. E. Comings, and O. S. Alfi (1977) *Chromosoma (Berl.)* **60,** 15–25.
7. M. L. Barcellona, R. Favilla, J. von Berger, M. Avitabile, N. Ragusa, and L. Masotti (1986) *Arch. Biochem. Biophys.* **250,** 48–53.
8. M. L. Barcellona and E. Gratton (1989) *Biochim. Biophys. Acta* **993,** 174–178.
9. M. L. Barcellona and E. Gratton (1990) *Eur. Biophys. J.* **17,** 315–323.
10. A. G. Szabo, D. T. Krajcarski, P. Cavatorta, L. Masotti, and M. L. Barcellona (1986) *Photochem. Photobiol.* **44,** 143–150.
11. M. J. Wirth and H. O. Fatunmbi (1990) *Anal. Chem.* **62,** 973–976.
12. B. E. Anderson, R. D. Jones, A. A. Rehms, P. Ilich, and P. R. Callis (1986) *Chem. Phys. Lett.* **125,** 106–112.
13. A. A. Rehms and P. R. Callis (1987) *Chem. Phys. Lett.* **140,** 83–89.
14. R. R. Birge, L. P. Murray, B. M. Pierce, H. Akita, V. Balogh-Nair, L. A. Findsen, and K. Nakanishi (1985) *Biophys.* **82,** 4117–4121.
15. R. R. Birge (1986) *Acc. Chem. Res.* **19,** 138–146.
16. J. R. Lakowicz and I. Gryczynski (1992) *Biophys. Chem.*, in press.
17. W. Denk, J. H. Strickler, and W. W. Webb (1990) *Science* **248,** 73–76.
18. W. W. Webb (1990) *MICRO '90*, London. pp. 445–450.
19. D. W. Piston, D. R. Sandison, and W. W. Webb (1992) *SPIE* **1640,** 379–389.
20. J. R. Lakowicz, H. Szmacinski, K. Nowaczyk, and M. L. Johnson (1992) *Proc. Natl. Acad. Sci. USA* **89,** 1271–1275.
21. R. Clegg, B. Fedderson, E. Gratton, and T. M. Jovin (1992) *SPIE* **1640,** 448–460.
22. J. R. Lakowicz, H. Szmacinski, K. Nowaczyk, K. Berndt, and M. L. Johnson (1992) *Anal. Biochem.* **202,** 316–330.

23. W. D. Wilson, F. A. Tanious, H. J. Barton, L. Strekowski, and D. W. Boykin (1989) *J. Am. Chem. Soc.* **111,** 5008–5010.
24. J. R. Lakowicz (1983) *Principles of Fluorescence Spectroscopy,* Plenum Press, New York.
25. J. R. Lakowicz, G. Laczko, and I. Gryczynski (1986) *Rev. Sci. Instrum.* **57,** 2499–2506.
26. G. Laczko, I. Gryczynski, W. Wiczk, H. Malak, and J. R. Lakowicz (1990) *Rev. Sci. Instrum.* **61,** 2331–2337.
27. J. R. Lakowicz, I. Gryczynski, and E. Danielsen (1992) *Chem. Phys. Lett.*, **191,** 47–53.
28. J. R. Lakowicz, I. Gryczynski, Z. Gryczynski, E. Danielsen, and M. J. Wirth (1992) *J. Phys. Chem.* **96,** 3000–3006.
29. W. M. McClain (1972) *J. Chem. Phys.* **57,**:2269–2272.
30. T. W. Scott, K. S. Haber, and A. C. Albrecht (1983) *J. Chem. Phys.* **78,** 150–157.
31. H. Sato, M. Kawasaki, and K. Kasatani (1984) *Chem. Phys.* **83,** 451–460.
32. G. Weber (1966) in D. M. Hercules. (Ed.), *Fluorescence and Phosphorescence Analysis*, J. Wiley and Sons, New York. pp. 217–240.
33. T. Kobayashi and S. Nagakura (1972) *Chem. Phys. Lett.* **13(3),** 217–220.
34. S. M. Kennedy and F. E. Lytle (1986) *Anal. Chem.* **58,** 2643–2647.
35. R. G. Freeman, D. L. Gilliland, and F. E. Lytle (1990) *Anal. Chem.* **62,** 2216–2219.
36. J. Papenhuijzen and A. J. W. G. Visser (1983) *Biophys. Chem.* **17,** 57–65.
37. B. P. Maliwal and J. R. Lakowicz (1986) *Biophys. Acta* **873,** 161–172.
38. J. R. Lakowicz, I. Gryczynski, E. Danielsen, and J. Frisoli (1992) *Chem. Phys. Lett.*, **194,** 282–287.